Measuring degradation of bonded insulated rail joints

Daniel Peltier, Graduate Research Assistant in Civil and Environmental Engineering

Christopher P. L. Barkan, Associate Professor in Civil and Environmental Engineering

Steven Downing, Visiting Lecturer in Mechanical Science and Engineering

Darrell Socie, Professor Emeritus in Mechanical Science and Engineering

Newmark Civil Engineering Lab

1205 N. Mathews Ave.

University of Illinois at Urbana-Champaign

Urbana, IL 61801

ABSTRACT

Degradation and failure of insulated joints (IJ's) is a major railroad maintenance problem today. Current techniques for monitoring IJ condition and detecting defects are either too labor-intensive for everyday use or too inaccurate for efficient planning of IJ replacement. While it is nontrivial to directly measure the extent of problems such as epoxy debonding or loss of resistance, such degradation also causes other, more measurable changes in certain properties of the joint. For instance, loss of epoxy bonding near the endpost changes the strain distribution within the joint bars.

This paper describes several ways in which simple measurements of such properties can be correlated with common joint problems. The emphasis is on properties that can be measured using inexpensive, fully automatic monitoring systems. The potential application of "smart sensors" (wireless, self-contained, auto-networking measurement devices) and other technology is discussed.

Computer modeling and laboratory testing have confirmed that the strain response of an IJ changes as the epoxy layer debonds from the metal surfaces. Field testing will be conducted to verify that these changes can be reliably detected and distinguished from the normal variation experienced by a healthy joint.

Tests to date also suggest that simple voltage measurements, collected automatically and without interference to track circuit operation, could give an indication of intermittent failure in the joint's insulating capability.

1. INTRODUCTION

Insulated rail joints (IJ's) are widely used throughout the North American rail network. Most mainline track uses "bonded" or "glued" IJ's, in which the insulator separating the joint bars from the rails is embedded in a strong epoxy, which binds the joint bars to the rails and allows minimal relative movement. Although bonded IJ's have been shown to have greater stiffness than unbonded ones (*1*), they still have shorter service lives than most other track components, especially on lines with dense traffic and high axle loads (*2*). The most common cause for replacement of a bonded IJ is a sustained or intermittent loss of electrical resistance between the two rail segments. This loss of insulating ability can lead to a fail-safe loss of signaling information and disruption of rail operations.

Before failing electrically, bonded IJ's often suffer from mechanical degradation that allows increased deflection, prevents them from distributing loads effectively across the substructure, and results in localized damage to the track structure (*2*). A mathematical model for the performance of a bonded IJ in track exists (*3*), but the impact of debonding on tie loads has not been quantified due in part to the difficulty of measuring debonding.

The Association of American Railroads, insulated joint suppliers, universities, and railroads are seeking ways to extend joint life through improved joint designs, materials, and support configurations (*4,5*). A complementary approach to the problem is to mitigate the disruptiveness of joint degradation and failure by detecting problems sooner, allowing more flexibility in scheduling joint replacement.

This paper discusses new ways to measure, evaluate, and monitor the condition of bonded insulated joints. The goal is to find nondestructive methods for detecting common

problems that can be built into an automated condition monitoring system, with the resulting data used for maintenance planning.

2. PROBLEM DESCRIPTION

2.1 Joint Distress and Failure

Davis et al. (*2*) identify a sequence of events representing "the most typical failure scenario of bonded IJ's in HAL service." This sequence starts with part of the epoxy layer debonding from the rail, joint bar, or both. Debonding begins at the endpost and slowly extends outward towards the vertical edges of the joint. The joint gets looser and looser, with increased vertical deflections, poorer load distribution, and relative component motion. Additionally, debonding allows water to penetrate the joint and rust the interior metal surfaces.

Electrical failure often results when the loose joint experiences contact between metal surfaces on the rails and joint bars or bolts – a result of fretting, deterioration or wear in the insulator, relative component movement, and related processes. The increased deflections caused by epoxy debonding can also cause mechanical distresses sufficient to condemn the joint, such as a broken bolt, cracked joint bar, or a "pull-apart" in which longitudinal tension and insufficient bond strength combine to cause plastic slippage between rail and joint bar. Even before the joint "fails", debonding can lead to load concentrations and localized ballast degradation.

2.2 Existing Inspection Techniques

2.2.1 Electrical Inspection

Electrical inspection of an insulated joint consists of testing the joint's ability to prevent electrical current from flowing from one track circuit to the other. The AREMA C&S manual includes two techniques for measuring the electrical soundness of a joint (*6*). Both tests involve shunting around one joint to test the soundness of the opposite joint. This means that a positive result (failed IJ) will lead to a temporary signal failure (until the shunt is removed), and therefore requires track time.

S&C Distribution Company sells a device called a "Track Circuit Short Finder" that can also be used to test the electrical soundness of an insulated joint (*7*). This device applies an alternating voltage to test IJ impedance. The frequency of the applied voltage is designed to prevent the resulting AC current from interfering with track circuit operation.

A disadvantage of these techniques is that they only provide information about the soundness of the joint at a single point in time. Catching intermittent failures requires an automated, leave-in-place system. Although the technology used in the S&C short finder could conceivably be adapted to form the basis of a continuous monitoring system, signal engineers might be justifiably nervous about an unmanned circuit monitoring system that constantly applies a voltage to the rails.

2.2.2 Visual inspection

FRA regulations now require visual inspections of IJ's in continuous welded rail once or twice a year (*8*). Such inspections must look for joint bar cracks, broken or missing bolts, rail end batter, and evidence of longitudinal movement.

An inspector can also examine the edge of the epoxy / insulator layer, which is visible between the rail and joint bar. Large relative deflections between rail and bar often cause this edge to crack or break away. Thus, it is possible to see some evidence of a joint that is loosening due to epoxy debonding. However, epoxy debonding occurs mostly on surfaces that are not visible to the inspector, making it impossible to quantify epoxy debonding through visual inspection.

2.3 Principles for Improved Monitoring Techniques

Existing inspection techniques have two main weaknesses:

1.) They must be conducted manually, and cannot easily be automated.

2.) They don't provide much information about two common problems, intermittent electrical failure and epoxy debonding.

The University of Illinois is investigating two new approaches to evaluating IJ condition, one for intermittent electrical failure and one for epoxy debonding. In both cases, the emphasis is on techniques that can be economically implemented in a non-vital, fully-automated continuous monitoring system. These approaches are intended for maintenance planning, rather than safety assurance.

3. MONITORING FOR INTERMITTENT ELECTRICAL FAILURES

3.1 Voltage-based Electrical Testing of an Insulated Joint

Figure 1 shows a simplified diagram of two adjacent DC track circuits. Track occupancy is detected via an electrical relay (TR) or its solid-state equivalent, so the primary quantity of concern is electrical *current*. An insulated joint causes signal failure when

electrical current flows through it. Current can only flow when joint resistance is low, so resistance is another critical value. Unfortunately, it is difficult to measure current or resistance unobtrusively.

The voltage between two parts of a circuit, on the other hand, is quite easy to measure without affecting the circuit's operation. The relationship between voltage and current or resistance is often fairly straightforward, although an indirect, voltage-based approach will probably not detect failure in all situations.

3.2 Theory

For analyzing DC track circuits (including Electrocode-type coded circuits), the fundamental equation is Ohm's Law: $I = V / R$, where I = current, V = voltage, and R = resistance.

Consider the pair of adjacent track circuits shown in Figure 1. If the resistance of IJ_1 drops to a very low value but the resistance of IJ_2 stays high, current flow is unaffected. No current flows across IJ_1 because that current would have no return path. So at IJ_1 the current I and the resistance R are both very low. Ohm's law says that the voltage across the failed joint (the voltage between **B** and **E**) must also be very low.

If both joints fail, current will flow directly from the track battery through the adjustable resistor, into the rail, through the bad joint, and into the opposite terminal of the other track battery (paths **ABE** and **DFC**). Ignoring the resistance of the rail itself, this alternative path has two resistors in series: the relatively high resistance of the adjustable resistor, and the relatively low resistance of the failed IJ. Ohm's Law says that the ratio of the voltages across the two resistors is equal to the ratio of the two

resistances. In other words, the voltage across the failed IJ will be very low regardless of the condition of the other joint.

Low voltage is not always indicative of a failed joint – the presence of a train could also cause a low voltage on one or both joints. (A case in which the adjacent circuits have the same polarity might also have low joint voltage under normal conditions, but signal engineers usually try to avoid such situations.) So the precise qualitative prediction made by this analysis is that a low voltage across an insulated joint *when no trains are present in the adjacent blocks* indicates low IJ resistance.

Note that this analysis ignores any AC voltages in the track. But Ohm's Law applies to these voltages as well (with some modification due to the dynamic property known as inductance). If a time-average of the absolute value of the voltage is used as the criterion, then it is still true that a low voltage is indicative of low resistance.

3.3 Field Testing

Tests were conducted on four installed IJ's at two locations on Class I mainline track. One pair of joints (joints B_1 and B_2) was located at an intermediate block signal between two coded track circuits. The second pair (C_1 and C_2) was at a control point, separating a coded circuit from a straight DC circuit. In each case, a signal maintainer had previously marked one of the joints (B_2 and C_2) for removal based on a visual and / or electrical inspection, but no signal problems had been reported. Using a Somat 2100 field data logging unit with a high-resistance (600 kΩ) voltmeter, a short time / voltage plot was taken across each of the four joints. In no case did the voltmeter cause any measurable change in current at the track relay.

The results, along with moving averages of the absolute value of the voltage, are shown in Figure 2. Note that the voltmeter cut off readings at +/- 2 V, but it is still possible to see the code pulses, the constant DC voltage (if any), and significant AC noise reflected in the cross-joint voltages. However, it is quite clear that no voltage ever develops across joint B_2. According to the logic in the previous section, these data imply that B_2 is failing to insulate the two track circuits, while the other three (including joint C_2, marked for removal by a signal maintainer) are still providingadequate insulation. These results were confirmed by testing using an S&C short finder and the shunt tests from the AREMA C&S manual.

3.4 Proposed Implementation

The implementation of a voltage-monitoring system is simplified by the fact that there are usually cables running from the signal cabinet to the four rail ends. The monitoring system can also be located in the signal box, and can tap into these cables. In fact, the voltage monitoring equipment could be built into the signal circuitry itself. This would also simplify the check to see whether low joint voltage is caused by the presence of trains or other shunts within the track circuits.

When a low joint voltage is detected, the news of a potential insulated joint failure can be communicated using wayside communications systems, broadcast over a wireless network for reading by a passing track inspector, or indicated within the signal cabinet, for a signal maintainer to check at his convenience.

4. EVALUATING EPOXY DEBONDING

4.1 Using Thermal Strain to Understand Condition

There are many mechanical properties of the joint that change as the epoxy layer comes debonded from the metal surfaces. Unfortunately, the most critical properties (such as deflection under a given load) are hard to measure in an economical, reliable, and automated manner.

On the other hand, one of the easiest mechanical properties to measure is the strain (or, equivalently, relative displacement) produced between two spots on the exterior of the joint. Strain gauges have no moving parts, and if properly protected from the elements they can achieve long life with no maintenance. In fact, strain gauges are already used for monitoring railroad track condition: they form the basis of the Salient Systems StressNet™ product, which detects changes in rail neutral temperature over time (*9*).

Strain is simply the reaction of a material to change in stress or load. For an automated monitoring system, it would be impractical to impose known loads in order to measure the resulting strain. The strain in response to some normally-occurring load must be the basis of the condition analysis.

An insulated joint is normally subjected to two major kinds of loadings: wheel loads from passing trains, and longitudinal loads from changes in rail temperature. Wheel loads are complicated, because the dynamic load of a rail car, including impact factor, can vary widely. Furthermore, the strain response of the joint can change daily due to uncontrolled, unmeasured variables such as support modulus. The load / strain relationship for longitudinal forces is a more reliable metric, because these forces develop slowly and depend on fewer uncontrolled variables.

The proposed method for evaluating epoxy debonding is therefore based on measuring changes in the strain response of a joint to thermal loads over time. This leads to the questions addressed in the next few sections: how can strain be efficiently measured in an insulated joint, how does epoxy debonding change the strain response of an IJ to thermal loads, and where should strain gauges be placed to detect these changes?

4.2 Smart strain gauges

Strain gauges are not always easy to install or configure, but next-generation wireless sensor technology has the potential to mitigate this problem. At the University of Illinois, researchers are designing a so-called "smart" strain gauge that combines a strain-sensing element, bridge, microprocessor / data logger, low-power Zigbee® radio, power source, and auto-configuring network software in a single wireless package (Figure 3).

Each gauge has two mounting points that can be attached to a surface in any manner desired. For a member that is thin in one dimension (such as the base of a rail), the sensor can be clamped on with C-clamps. For larger members, threaded pins can be attached to the surface (e.g. by using a capacitor-discharge stud welder) and the mounting points screwed down against the surface with nuts, as shown in Figure 3.

Data collection programs can be preloaded onto the on-board processor. After mounting, the sensors automatically join together into a network, with little further configuration required. The components are all commodity parts, and assembly can (theoretically) be automated, resulting in a device that is both inexpensive to manufacture and easy to install.

The Zigbee network is designed for extremely low power consumption rather than long ranges or low latency. That makes it perfect for communication among the sensors, but a gateway between this network and a dedicated wayside link or a more powerful wireless network would be required to communicate with maintenance personnel. Fortunately, such a gateway could usually be housed in a nearby signal cabinet and still be within Zigbee radio range.

4.3 Finite Element Modeling of IJ Strains with Epoxy Debonding

Smart strain gauges provide the technology needed to measure strains in the joint. To make use of these measurements requires an understanding of how strain response changes in a deteriorating joint. Finite element analysis gives some suggestions, and laboratory tests to confirm these results are discussed in the next section.

4.3.1 Model Description

Two finite element models of 36RE bonded insulated joints were used to study strain response. The models represent conventional insulated joint plugs manufactured by two leading IJ suppliers. Both use 36-inch joint, 6-hole joint bars, with the primary difference being the shape of the bar. Both models were created using the MSC.Patran 2005 software program, and analyzed with ABAQUS 6.4.

The rails and joint bars were modeled using 10-node tetrahedron solid elements having typical material properties of carbon steel. The insulating epoxy layer consisted of a single layer of 10-node tetrahedra, with material properties based on standard industrial epoxies and technical advice from IJ researchers. The bolts and endpost were assumed to

carry little to no load under the small deformations involved in the study, and were not included. This decision may limit the accuracy of the model when extensive debonding allows the rail to move enough to bear on the bolts. The bolt *holes* are included, as they affect stress distribution within the joint bars even for a fully bonded joint.

The epoxy and steel were connected using contact surfaces. For a fully bonded joint, these contact surfaces were "tied", meaning nodes on both sides of the interface experience equal displacements. Debonded areas were modeled with "general" contact surfaces, which allow the two sets of nodes to slip tangentially or separate in the normal direction. No frictional forces were included at the debonded surfaces.

The applied load consisted of a longitudinal tensile force applied to one end of the joint plug through the rail's neutral axis. This kind of loading would result from a decrease in rail temperature.

4.3.2 Finite Element Results

Figure 4 shows a progression representing the strain distribution under a 40 kip tension load as debonding spreads outward from the endpost. There are three features of the strain response worth noting:

1.) The strain at the center of the joint bar increases with increased debonding, up to a certain point.

2.) The strain near the ends of the joint bar does not change much for moderate debonding, but increases when the debonded area gets very large.

3.) The amount by which the gap between rails opens up under load increases with increased debonding.

4.3.2.1 Strain at Joint Bar Center Tensile strain at the center of the joint bar becomes larger as debonding progresses. Simple static analysis says that the total tensile load carried by the joint bar at the joint center is the same regardless of debonding – it must be equal to ½ of the total 40 kip load. So the apparent increase must be caused by a change in how the tensile stress is distributed across the cross-sectional face of the joint bar. Figure 5 shows how the strain distribution through the joint bar cross-section at the center of the joint changes with debonding. While debonding does not affect the average tensile strain at the center of the joint bar, it does tend to increase the strain *at the outside surface*, where a strain gauge could feasibly be placed.

When the debonded area extends past a certain point, the stress distribution will equalize across the joint bar cross section and the strain on the outer surface will not increase with further debonding.

4.3.2.2 Strain Near End of Joint Bar The predicted tensile strain on the outside surface of the joint bar near the ends (for instance, halfway between the first and second bolt holes) does not change nearly as much as the strain at the center of the joint bar for small amounts of debonding. On the other hand, when the debonding spreads over a very large percent of the joint (such as in Figure 4.f), the strain near the end of the joint bar can increase substantially.

4.3.2.3 Gap Opening Figure 6 shows the deformation of an IJ under the same load and debonding patterns as before (magnified by a factor of 1000). Note that even in a fully-

bonded joint the gap between the rails will open up by a small amount when tension is applied. As epoxy debonding progresses, this gap opening gets larger and larger. This does not represent a "pull-apart": the joint is not slipping, but the elastic deformation is increasing. While the gap opening is not technically a "strain" quantity, it is a relative displacement of two parts of the system. It can be measured easily with an extensometer, which is more or less equivalent to a strain gauge.

4.4 Laboratory Testing of Strain Response

An IJ testing program is being conducted at the Newmark Structural Engineering Laboratory at the University of Illinois at Urbana-Champaign. The goal of this testing is to measure the differences in strain response of insulated joint plugs with differing amounts of epoxy debonding when tensile loads are applied.

4.4.1 Test Specimens

Three bonded insulated rail joint plugs have been tested to date:

- NEW_A: A newly manufactured joint from Supplier A. This specimen is assumed to have no epoxy debonding.
- OLD_A: A used joint from Supplier A that appears to have suffered a "pull-apart", implying poor bond strength and extensive debonding.
- OLD_B: A joint manufactured by Supplier B and removed from track due to an unknown failure. Visual inspection reveals that the edges of the epoxy layer have debonded from the rails over several inches.

All specimens use 36-inch joint bars with conventional hole spacing and 136RE rail.

4.4.2 Test Setup

4.4.2.1 Test apparatus The specimen plugs are cut to a length of 11 feet, placed horizontally between a servohydraulic actuator and a reaction block, and attached with a single bolt through the rail neutral axis on each end. The design load capacity of the apparatus is 50 kips. Because of play in the connections, data at loads below about 5 kips is highly variable and considered unreliable.

4.4.2.2 Instrumentation The names and locations of strain gauges and extensometers are shown in Figure 7. The "extensometers" are in fact smart strain gauges as described in section 4.2, with the two mounting points attached to the two different rails. In addition, three strain gauges are placed on each of the two rail segments outside the joint bar to measure the actual load delivered by the test apparatus.

4.4.3 Results and Analysis

The analysis focuses exclusively on data in the range from 8 to 48 kips. This 40 kip range is roughly equivalent to the load caused by a 15°F decrease in rail temperature. For the fully-bonded joint, most measurements showed a linear response within this range.

The measured strains for each IJ and the predicted strains from the finite element model for a fully-bonded joint are shown in Table 1. All values are corrected to remove unintended bending moments measured in the rails.

4.4.3.1 Quantitative Accuracy of the Model For the one fully-bonded joint tested to date (NEW_P), the finite element model estimated the strain in the joint bar to within 10%. Measured joint bar strains were mostly higher than predicted. On the other hand, the gap opening measured in the tests was significantly lower (by about 35%) than the predicted value. This discrepancy may reflect the decision not to include the bolts in the model, or it may mean that the actual epoxy is stiffer than the model properties.

4.4.3.2 Qualitative Predictions Finite element analysis gives three qualitative predictions about the effects of debonding on strain response (see section 4.3.2). The test data from the two joints from Supplier A (NEW_A and OLD_A) allow for direct testing of these predictions. The evidence of a pull-apart suggests that the OLD_A joint probably has a large debonded area. Therefore, the strains at both the center and ends of the joint bars, as well as the elastic gap opening between rail ends, should be larger in OLD_A than in the fully-bonded NEW_A specimen. The results in Table 1 agree with this prediction: the joint bar strains are all roughly 50% higher, while the gap opening is 600% larger.

Because the specimens tested so far do not include a fully bonded joint from Supplier B, the OLD_B test results can only be compared to finite element predictions. Since visual inspection suggests a moderate amount of debonding, the strain in the joint bar center should be higher than for a fully bonded joint, the strain near the edges of the joint bar should be only a little bit higher, and the gap opening should be modestly larger.

The actual test results for OLD_B are somewhat more complicated. The gap opening results and the strain at the center of the joint bars are considerably higher on one

side of the joint than on the other. According to the finite element analysis, this situation can arise when debonding is more extensive on one joint bar than on the other, as implied by Figure 8. Averaging the strain and extension results over the two sides of the joint, the joint bar center strain in specimen OLD_B is almost 50% above the predicted value for a fully bonded joint, with a 27% larger increase in gap size.

On the other hand, strains near the edges of the joint bar are 30% higher than expected for a fully bonded joint. This difference is greater than expected for a joint with moderate debonding. There are at least two possible explanations: either the finite element predictions are not accurate for this joint design, or the OLD_B joint has more extensive debonding than the visual inspection would suggest. It is not possible to distinguish between these hypotheses given the test data collected to date.

4.6 Future Research

4.6.1 Future Laboratory Tests

Future laboratory tests will be directed towards two purposes: testing and revising the predicted effects of debonding on strain response, and applying smart strain gauge technology to measure IJ strains.

Building on previous tests, the project has acquired a new joint from Supplier B. Tests on this specimen will allow comparison to the OLD_B joint, so that the effects of debonding can be seen directly (as they are for the specimens NEW_A and OLD_A). In addition, other failed joint specimens will be tested to explore different debonding patterns. Finally, some failed joints will be broken apart to directly examine the shape

and extent of debonded areas, allowing the effects predicted by the finite element model to be compared quantitatively to the test strain results.

Future tests will make greater use of smart strain gauges for all measurements. Smart strain gauges have already been used as extensometers to measure gap openings, and have performed adequately. Gauges with a greater sensitivity will be needed to measure strains within the joint bar itself, with correspondingly tougher requirements for secure and precise attachment of the mounting points.

4.6.2 Field Tests

Laboratory testing can provide an understanding of joint strain response to pure tension loads, but the loading environment in railroad track may not be so simple. In addition, the supply of joint specimens available for lab testing is mostly limited to joints that have passed the point of incipient debonding and progressed to complete failure of some kind. To address these problems and avoid the difficulty of deploying conventional strain gauges in the field, smart strain gauges will be used to gather field data on in-track joints with varying accumulated tonnage.

An initial round of tests at the Transportation Technology Center test track in Pueblo, CO will provide single-point-in-time data from several existing IJ's. These tests will consist of temporarily instrumenting a joint and gathering data over several thermal cycles (days). In a later round of testing a new instrumented IJ will be installed in the test track. Changes in strain response as traffic accumulates will be compared to visual evidence of joint distress.

5. CONCLUSIONS

Insulated joint failure causes significant disruptions to railroad operations. Better information about insulated joint condition can allow for improved IJ replacement planning. Ongoing research has identified several promising approaches for identifying common insulated joint problems with better reliability, earlier warning, and less human intervention than existing inspection techniques.

An insulated joint with an electrical failure can sometimes be identified by a drop in the voltage between the two rails of the joint. This voltage can be measured without disrupting the track circuit. Intermittent failures can be noticed by a system that constantly samples this voltage value and watches for sudden drops.

Epoxy debonding can be detected by applying smart strain gauges to certain locations on the joint. These strain gauges measure certain salient characteristics of the joint's response to thermal stresses that change as epoxy debonding progresses outwards from the endpost. Finite element modeling and laboratory testing have identified increases in the strain at the center of the joint bar and the elastic gap opening between rail ends as salient characteristics of debonding.

Future research will include field tests of strains in an in-track insulated joint and prototype implementations of a smart strain gauge system for measuring joint strains.

ACKNOWLEDGEMENTS

This project is sponsored by a grant from the Association of American Railroads under the Strategic Research Initiative and Technology Scanning programs. The first author was supported partly by a CN Railroad Engineering Fellowship. David Davis and

Muhammad Akhtar of Transportation Technology Center, Inc. provided assistance and technical guidance.

Additional material and technical assistance was provided by Norfolk Southern Corporation; Portec Rail; Allegheny Rail Products (a division of L. B. Foster Co.); BNSF Railway; and CN.

REFERENCES

(1) Cox, Joel E. *Rail Joint Mechanics*. Master's Thesis, Department of Civil Engineering, University of Delaware, 1993.

(2) Davis, D. D.; Akhtar, M.; Kohake, E.; and Horizny, K. Effects of heavy axle loads on bonded insulated joint performance, *Proceedings of the AREMA 2005 Annual Conference*, Chicago, IL, 2005.

(3) Kerr, Arnold D. and Cox, Joel E. "Analysis and tests of bonded insulated rail joints subjected to vertical wheel loads," *International Journal of Mechanical Sciences*, v41, n 10, Oct, 1999, p. 1253-1272.

(4) Li, D.; Meddah, A.; Davis, D.; and Kohake, E. "Performance of insulated joints at western mega site," Transportation Technology Center, Inc. Technology Digest TD-06-28, December 2006.

(5) Akhtar, Muhammad N. and Davis, David D. "Preliminary results of prototype insulated joint tests at FAST," Transportation Technology Center, Inc. Technology Digest TD-07-13, May 2007.

(6) *2000 Communications & Signals Manual,* Part 8.6.35, The American Railway Engineering and Maintenance of Way Association, 2000.

(7) S&C Distribution Co. website:

http://www.sandcco.com/insulatedjointtesting.htm, accessed July 2, 2007.

(8) *United States Code of Federal Regulations*, Title 49, Section 213.119.g.

(9) Harrison, Harold. "Measuring the longitudinal forces in heavy haul track," *Proceedings: International Heavy Haul Conference Specialist Technical Session - High Tech in Heavy Haul*, Kiruna, Sweden, June 2007, p. 565-570.

LIST OF FIGURES

LIST OF TABLES

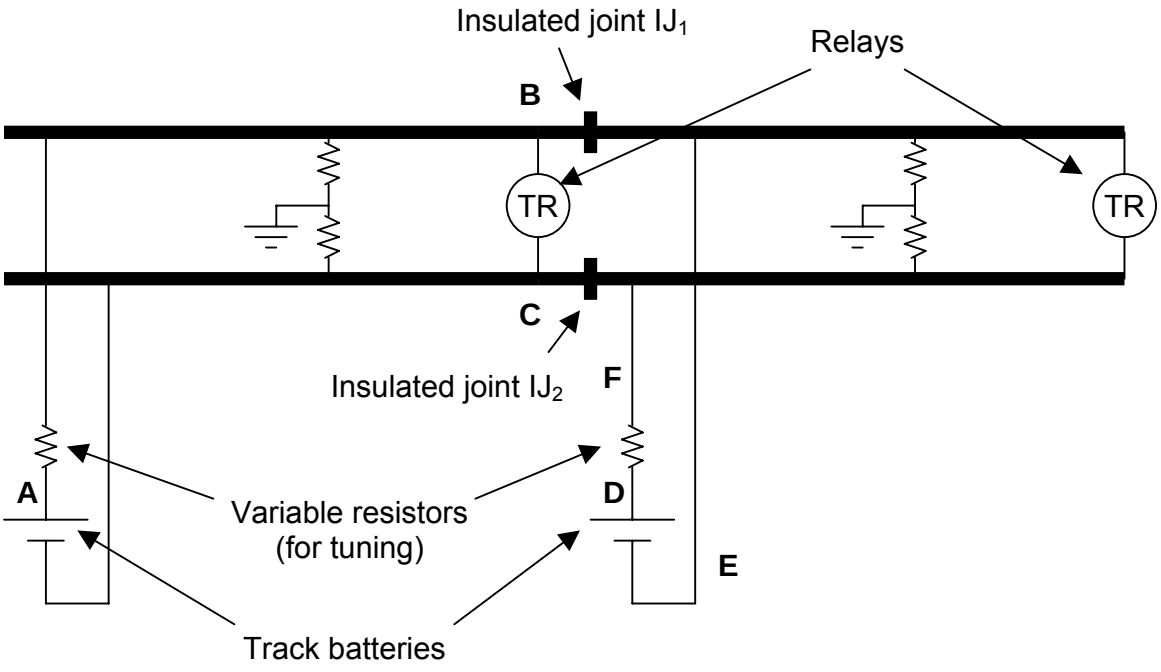

FIGURE 1: Simplified Diagram of Two DC Track Circuits

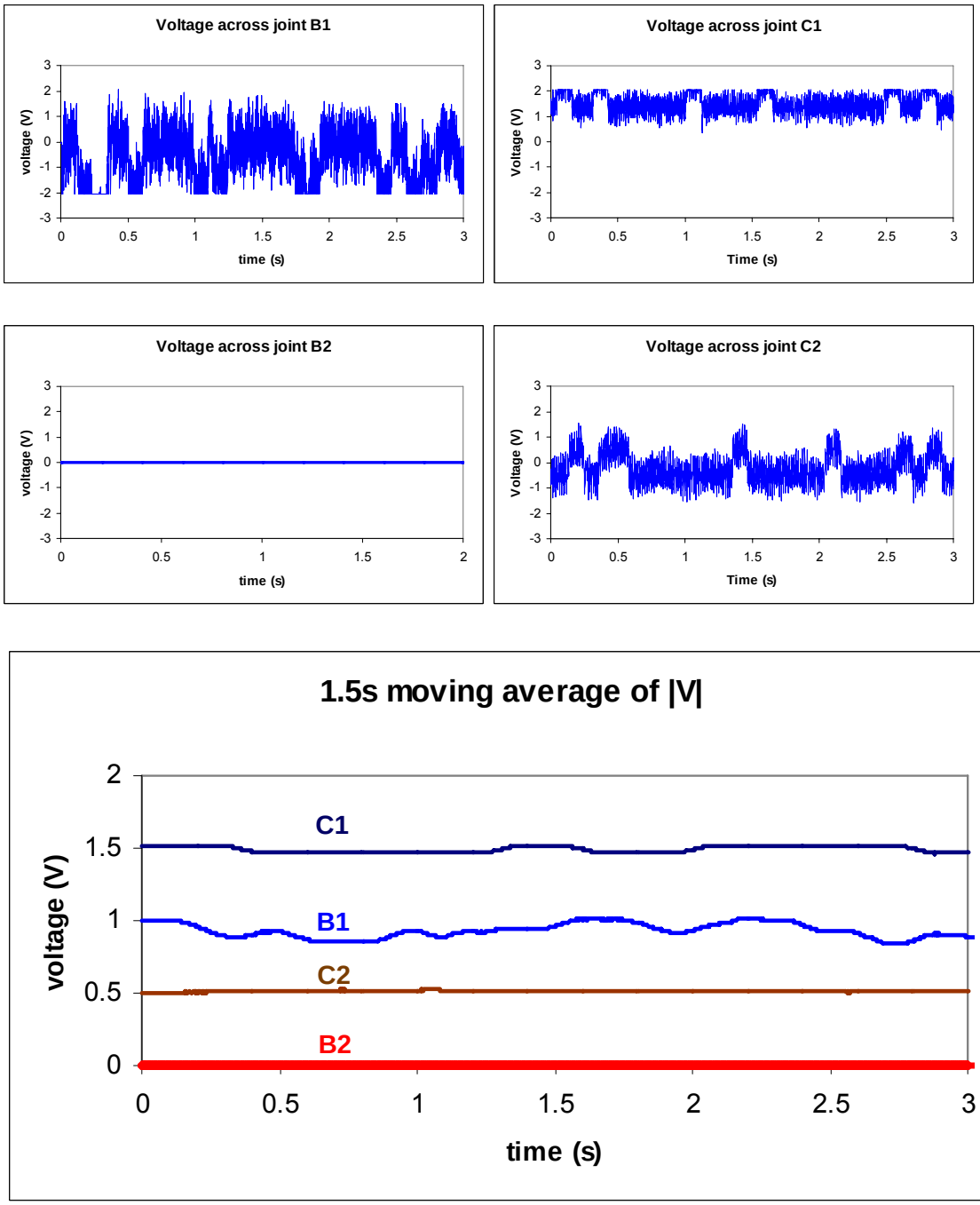

FIGURE 2: Measured Voltages across Four Insulated Joints

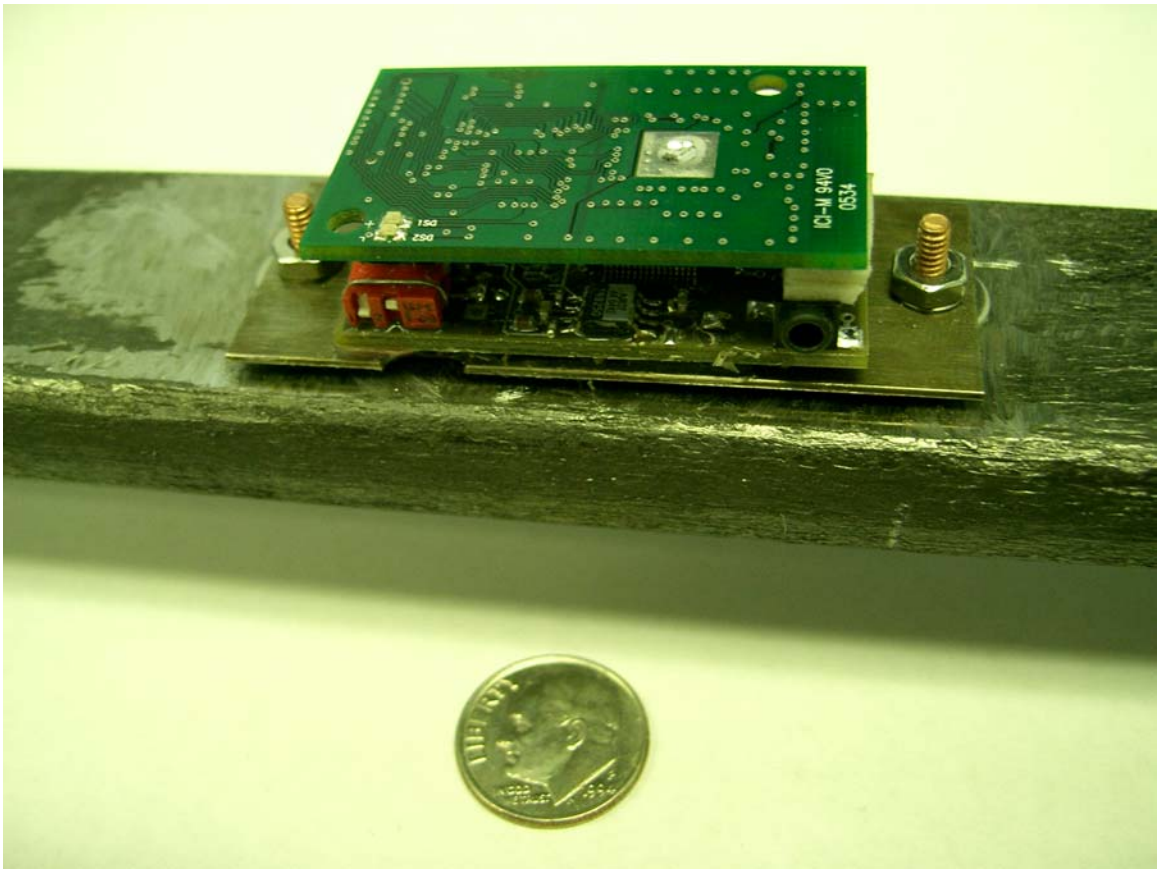

FIGURE 3: Smart Strain Gauge Mounted Using Welded Threaded Studs and Nuts

FIGURE 4.a: Fully Bonded Joint

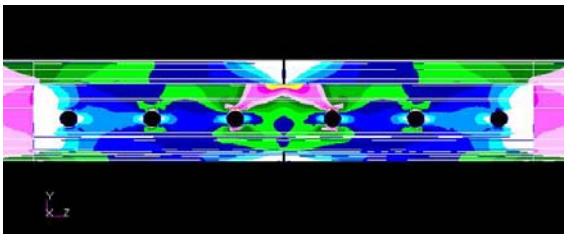

FIGURE 4.b: 1 Inch Debonded Area

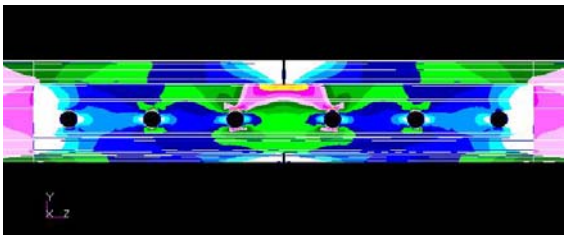

FIGURE 4.c: 2.5 Inch Debonded Area

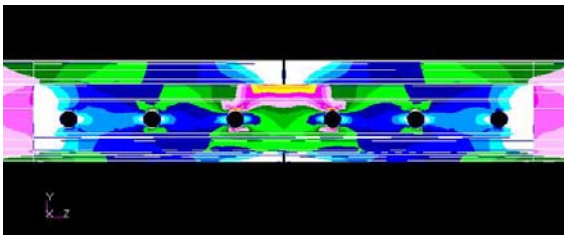

FIGURE 4.d: 4.5 Inch Debonded Area

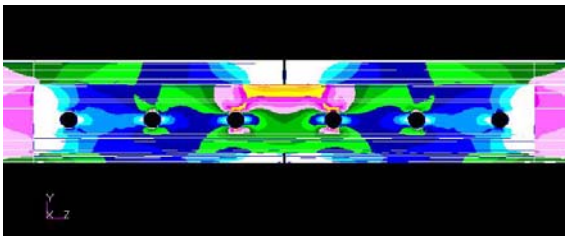

FIGURE 4.e: 7 Inch Debonded Area

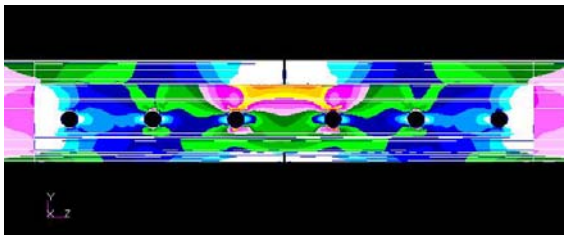

FIGURE 4.f: 19 Inch Debonded Area

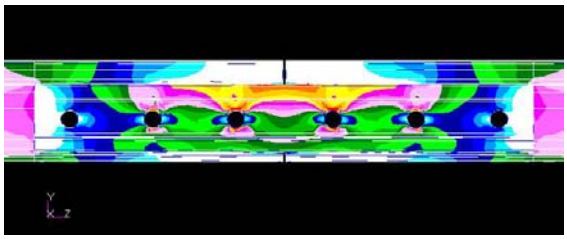

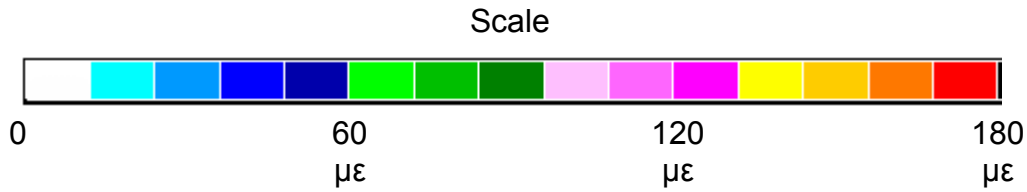

FIGURE 4: Longitudinal Strain under 40k Tension

FIGURE 5.a: Fully Bonded Joint

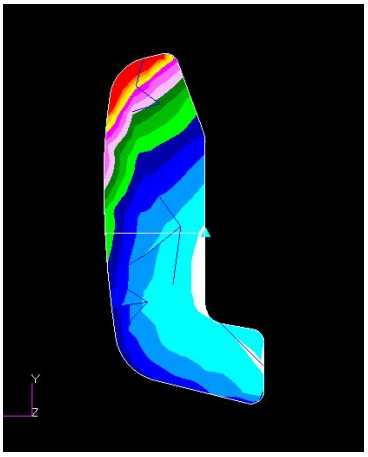

FIGURE 5.b: 1 Inch Debonded Area

FIGURE 5.c: 2.5 Inch Debonded Area

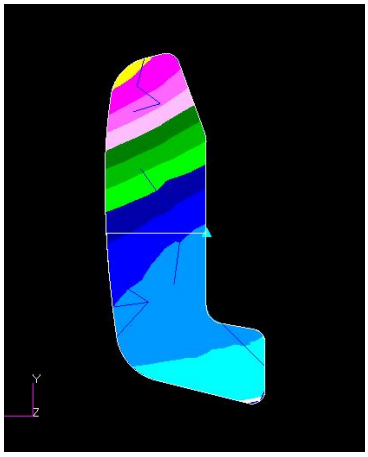

FIGURE 5.d: 4.5 Inch Debonded Area

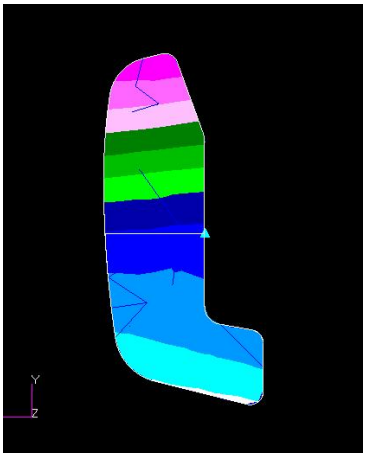

FIGURE 5.e: 7 Inch Debonded Area

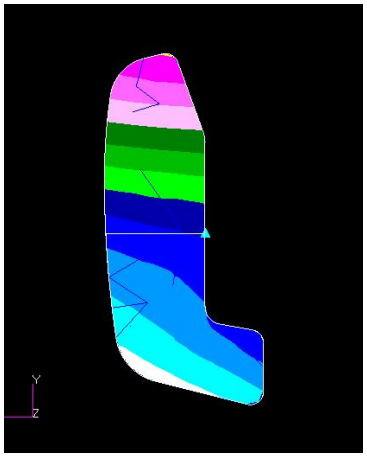

FIGURE 5.f: 19 Inch Debonded Area

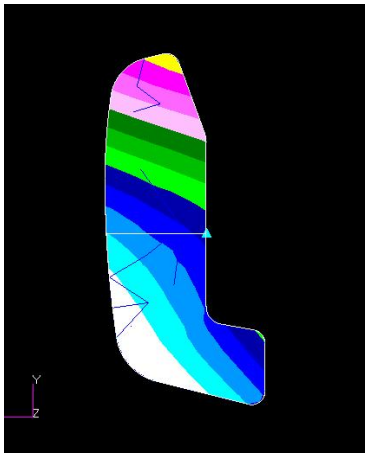

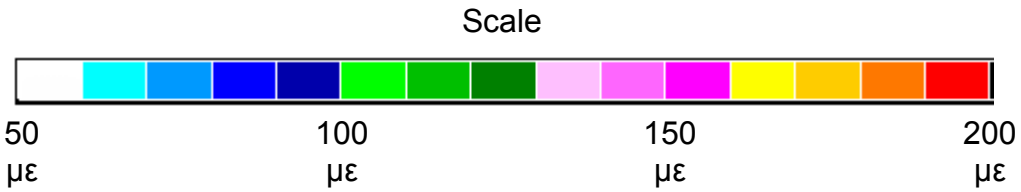

FIGURE 5: Longitudinal Strain at Center of Joint Bar under 40k Tension

FIGURE 6.a: Fully Bonded Joint

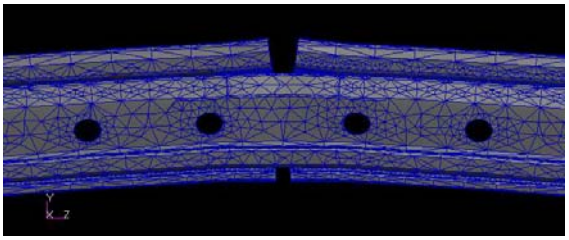

FIGURE 6.b: 1 Inch Debonded Area

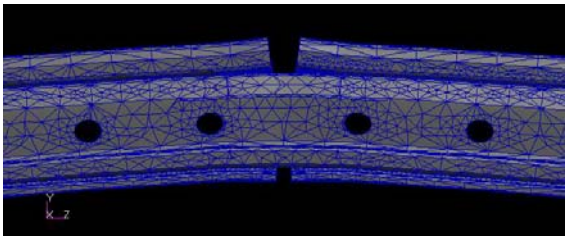

FIGURE 6.c: 2.5 Inch Debonded Area

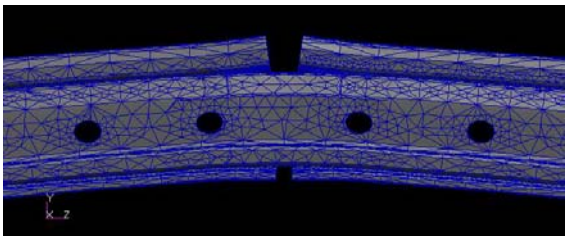

FIGURE 6.d: 4.5 Inch Debonded Area

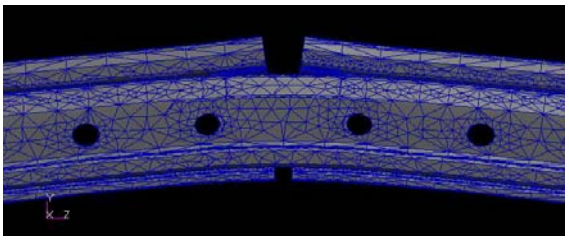

FIGURE 6.e: 7 Inch Debonded Area

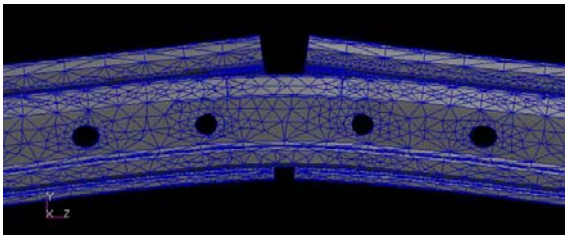

FIGURE 6.f: 19 Inch Debonded Area

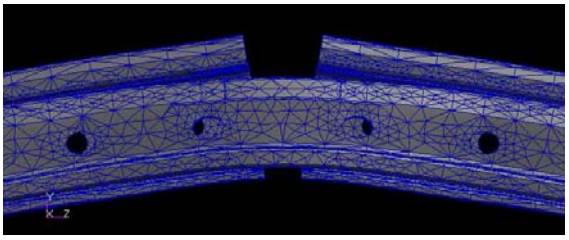

FIGURE 6: Deformation under 40k Tension (1000x Magnification)

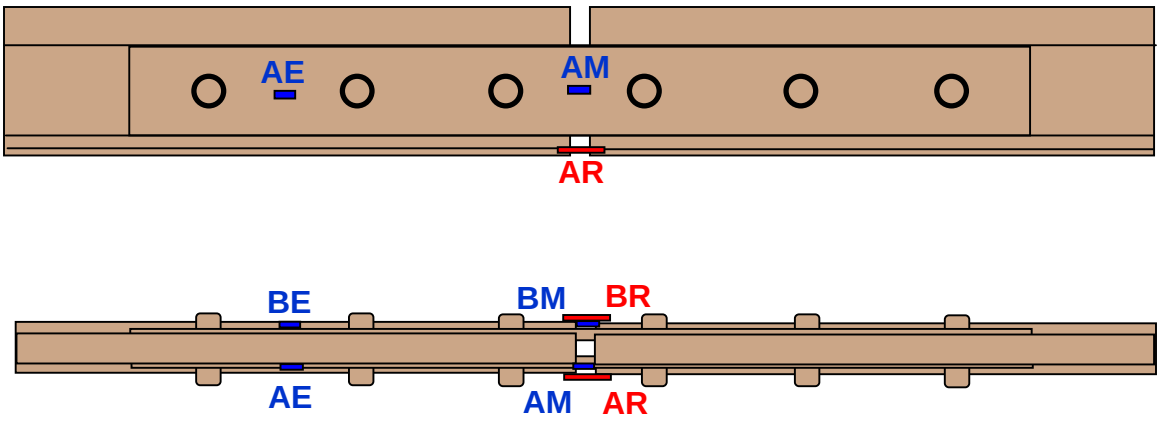

FIGURE 7: Location of Strain Gauges and Extensometers

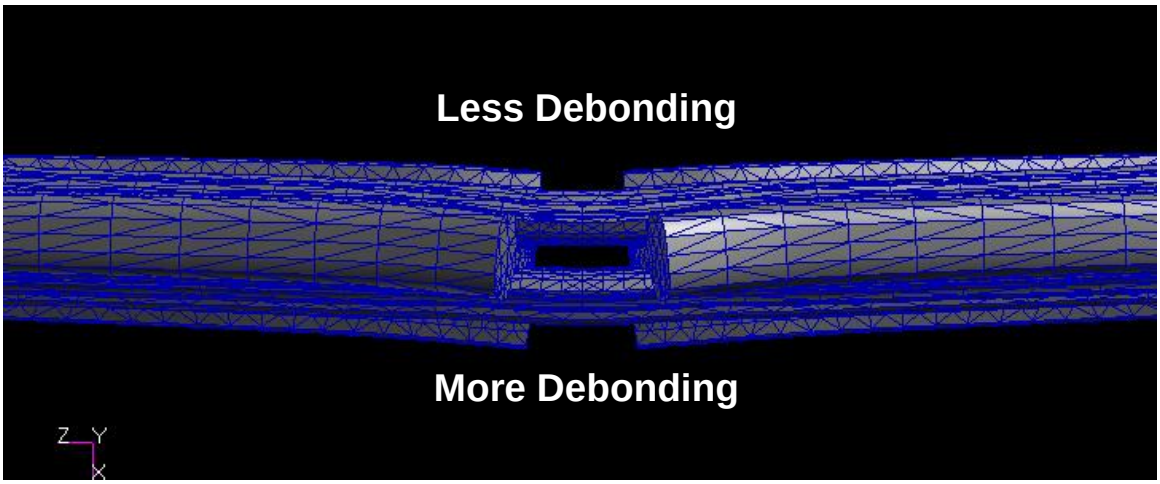

FIGURE 8: Deformation with Asymmetric Debonding (3000x Magnification)

Strain gauge / extensometer location	Supplier A			Supplier B	
	Prediction (full bond)	NEW_A	OLD_A	Prediction (full bond)	OLD_B
AM (με)	57	62	92	63	88
AE (με)	33	36	56	32	41
BM (με)	57	55	91	63	99
BE (με)	33	36	51	32	41
AR (μ-in)	540	340	2510	780	350
BR (μ-in)	540	N/A	N/A	780	1640

TABLE 1: Measured Strains under 40k Tension Load